# Deterioration Modeling of Steel Components in Support of Collapse Prediction of Steel Moment Frames under Earthquake Loading

Dimitrios G. Lignos, A.M.ASCE<sup>1</sup>; and Helmut Krawinkler, M.ASCE<sup>2</sup>

**Abstract:** Reliable collapse assessment of structural systems under earthquake loading requires analytical models that are able to capture component deterioration in strength and stiffness. For calibration and validation of these models, a large set of experimental data is needed. This paper discusses the development of a database of experimental data of steel components and the use of this database for quantification of important parameters that affect the cyclic moment-rotation relationship at plastic hinge regions in beams. On the basis of information deduced from the steel component database, empirical relationships for modeling of precapping plastic rotation, postcapping rotation, and cyclic deterioration for beams with reduced beam section (RBS) and other-than-RBS beams are proposed. Quantitative information is also provided for modeling of the effective yield strength, postyield strength ratio, residual strength, and ductile tearing of steel components subjected to cyclic loading. **DOI:** 10.1061/(ASCE)ST.1943-541X.0000376. © 2011 American Society of Civil Engineers.

CE Database subject headings: Deterioration; Steel; Databases; Residual strength; Earthquake loads; Steel frames; Failures.

**Author keywords:** Component deterioration; Steel database; Steel moment connections; Sidesway collapse; Moment-rotation relationships; Residual strength; Deterioration models; Reduced beam section.

#### Introduction

Significant progress has been made in recent years in methods to predict collapse under earthquake loading (e.g., Ibarra et al. 2002; Vamvatsikos and Cornell 2002; Ibarra and Krawinkler 2005; Haselton and Deierlein 2007; Zareian and Krawinkler 2009) and to develop engineering approaches for collapse protection (FEMA 2009; NIST 2010; Zareian et al. 2010). The collapse mode addressed in these studies is associated with sidesway instability in which *P*-Delta effects accelerated by component deterioration fully offset the first-order story shear resistance, and dynamic instability occurs. One of the primary challenges has been, and still is, the ability to reliably predict deterioration properties of structural components and to incorporate these properties into analysis tools.

Experimental studies have shown that the hysteretic behavior of structural components depends on numerous structural parameters that affect the deformation and energy dissipation characteristics, leading to the development of a wide range of versatile deterioration models. A summary of various hysteresis models developed during the 1960s and 1970s for reinforced concrete elements is presented in Otani (1981). More recently, Baber and Noori (1985), Casciati (1989), and Reinhorn et al. (1995) modified the widely known Bouc-Wen model (Bouc 1967; Wen 1980) to incorporate

Note. This manuscript was submitted on February 16, 2010; approved on December 27, 2010; published online on December 30, 2010. Discussion period open until April 1, 2012; separate discussions must be submitted for individual papers. This paper is part of the *Journal of Structural Engineering*, Vol. 137, No. 11, November 1, 2011. ©ASCE, ISSN 0733-9445/2011/11-1291–1302/\$25.00.

component deterioration. Song and Pincheira (2000) developed a model that simulates postcapping behavior but does not incorporate cyclic strength deterioration. Sivaselvan and Reinhorn (2000, 2006), on the basis of earlier models by Iwan (1966) and Mostaghel (1999), developed a smooth hysteretic model with stiffness and strength degradation and pinching characteristics, derived from inelastic material behavior. More recently, Ibarra et al. (2005) developed an energy-based phenomenological deterioration model that captures most important modes of component deterioration.

Reliable deterioration modeling of structural components requires validation of analytical models described previously with experimental data from components that have been subjected to various loading histories. Specific databases of experimental data are available for this purpose for reinforced concrete components [e.g., PEER database (Berry et al. 2004), http://nisee.berkeley.edu/spd] and in part for steel components (SAC database, http://www.sacsteel.org/connections/). The latter database does not include cyclic moment-rotation hysteresis diagrams, which are needed for the development of deterioration parameters of steel components.

In this paper, the primary focus is to provide information for the missing aspects of comprehensive modeling of the deterioration characteristics of structural steel components on the basis of a recently developed database that includes comprehensive data of more than 300 experiments on steel wide flange beams (Lignos and Krawinkler 2007, 2009). The experimental data is used to calibrate deterioration parameters of the phenomenological deterioration model summarized in the next section and to develop relationships that associate parameters of this deterioration model with geometric and material properties that control deterioration in structural steel components.

#### **Deterioration Model**

The deterioration model developed by Ibarra et al. (2005), referred to as Ibarra-Krawinkler (IK) model, forms the basis of the

<sup>&</sup>lt;sup>1</sup>Assistant Professor, Dept. Of Civil Engineering and Applied Mechanics, McGill Univ., Montreal, QC, H3A2K6 Canada (corresponding author). E-mail: dimitrios.lignos@mcgill.ca

<sup>&</sup>lt;sup>2</sup>Professor Emeritus, Dept. Of Civil and Environmental Engineering, Stanford Univ., Stanford, CA 94305.

deterioration modeling discussed in this paper. This model was modified by Lignos and Krawinkler (2009) to address asymmetric component hysteretic behavior, including different rates of cyclic deterioration in the two loading directions, residual strength, and incorporation of an ultimate deformation  $\theta_u$  at which the strength of a component drops to zero because of unstable crack growth and fracture.

The modified IK model establishes strength bounds on the basis of a monotonic backbone curve [see Fig. 1(a)] and a set of rules that define the characteristics of hysteretic behavior between the bounds [see Fig. 1(b)]. For a bilinear hysteretic response, three modes of cyclic deterioration are defined with respect to the backbone curve (basic strength, postcapping strength, and unloading/ reloading stiffness deterioration), as illustrated in Fig. 1(b). The model can be applied to any force-deformation relationship, but in this discussion is described in terms of moment and rotation quantities, as defined in Fig. 1. The backbone curve is defined by three strength parameters  $[M_v]$  = effective yield moment,  $M_c$  = capping moment strength (or postyield strength ratio  $M_c/M_v$ ), and residual moment  $M_r = \kappa \cdot M_v$ ] and four deformation parameters  $[\theta_v]$  = yield rotation,  $\theta_p$  = pre-capping plastic rotation for monotonic loading (difference between yield rotation and rotation at maximum moment),  $\theta_{pc}$  = post-capping plastic rotation (difference between rotation at maximum moment and rotation at complete loss of strength), and  $\theta_u$  = ultimate rotation capacity].

The rates of cyclic deterioration are controlled by a rule developed by Rahnama and Krawinkler (1993) on the basis of the hysteretic energy dissipated when the component is subjected to cyclic loading. It is assumed that every component has a reference hysteretic energy dissipation capacity  $E_t$ , which is an inherent property of the components regardless of the loading history applied to the component. The reference hysteretic energy dissipation capacity is expressed as a multiple of  $M_v \cdot \theta_p$ , i.e.:

$$E_t = \lambda \cdot \theta_p \cdot M_y$$
 or  $E_t = \Lambda \cdot M_y$  (1)

where  $\Lambda = \lambda \cdot \theta_p$  = reference cumulative rotation capacity; and  $\theta_p$  and  $M_y$  = precapping plastic rotation and effective yield strength of the component, respectively.

Cyclic strength deterioration (basic strength deterioration and postcapping strength deterioration) is modeled by translating the two strength bounds (the lines intersecting at the capping point) toward the origin at the rate

$$M_i = (1 - \beta_i) \cdot M_{i-1} \tag{2}$$

after every excursion i in which energy is dissipated. The moment  $M_i$  is any reference strength value on each strength bound line

(the intersection of the strength bound with the y-axis may be used for convenience), and  $\beta_i$  is an energy-based deterioration parameter given by

$$\beta_{i} = \left(\frac{E_{i}}{E_{t} - \sum_{j=1}^{i-1} E_{j}}\right)^{c} \tag{3}$$

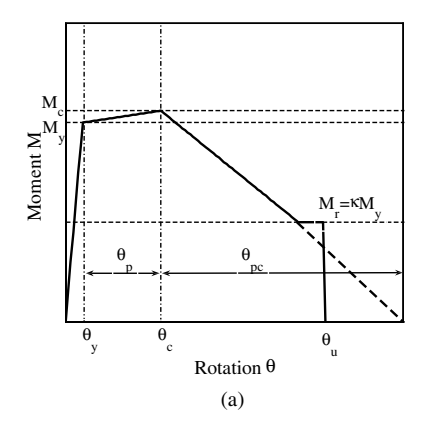
where  $E_i$  = hysteretic energy dissipated in excursion i;  $\Sigma E_j$  = total energy dissipated in past excursions;  $E_t$  = reference energy dissipation capacity from Eq. (1); and c = empirical parameter, usually taken as 1.0. Different rates of deterioration in the positive and negative direction, such as in the case of a beam with a composite slab, can be accommodated by multiplying the right-hand side of Eq. (3) by a parameter  $0 < D^{+/-} \le 1$ , which slows down the rate of deterioration in one direction and results in two different values of  $\beta$  in each direction (see Lignos and Krawinkler 2009).

The same concepts apply to modeling of unloading stiffness deterioration, i.e., the deteriorated stiffness after excursion i is given by

$$K_i = (1 - \beta_i) \cdot K_{i-1} \tag{4}$$

Different rates of deterioration for each cyclic deterioration mode can be incorporated by using different  $\Lambda$  values for each mode. Extensive calibration studies (Lignos and Krawinkler 2007, 2009) have shown that, for steel components, this refinement does not lead to significant model improvements. For more details on this deterioration model, see Ibarra et al. (2005) and Lignos and Krawinkler (2009).

For each experiment of the database discussed in the next section, parameters of the modified IK model were determined by matching the digitized moment-rotation response to a hysteretic response controlled by the backbone curve shown in Fig. 1 and a cyclic deterioration parameter  $\Lambda$ . A combination of engineering mechanics concepts and visual observations is employed to select appropriate parameters and pass judgment on satisfactory matching. For this purpose, an interactive Matlab-based tool was developed to automate the calibration process (Lignos and Krawinkler 2009). An example of a satisfactory calibration of the modified IK deterioration model is shown in Fig. 2 for two steel beams with and without composite action. Ma et al. (2006) and Yun et al. (2007) have used system identification and self-learning simulation for calibration of degrading systems with respect to experimental data. However, the use of visual observation and judgment (in addition to mechanics concepts) was found to be preferable to attempts to use rigorous approaches, such as a nonlinear least square optimization technique (Dennis 1977) and neural networks (Medsker and Jain 2000). The former was partially unsuccessful because of the



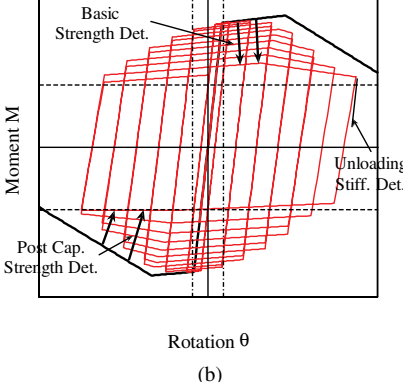


Fig. 1. Modified IK deterioration model: (a) monotonic curve; (b) basic modes of cyclic deterioration and associated definitions

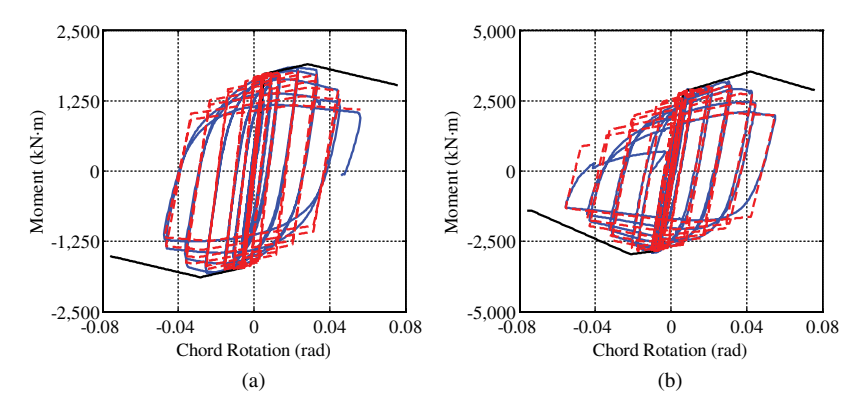


Fig. 2. Calibration examples of modified IK deterioration model: (a) beam with RBS (no slab, data from Uang et al. 2000); (b) asymmetric hysteretic response considering composite action (data from Ricles et al. 2004)

large number of variables, and the latter was found to be unreliable because the size of the steel database was too small to train the network.

The modified Ibarra-Krawinkler deterioration model has been implemented in DRAIN-2DX (Prakash et al. 1993) and Open System for Earthquake Engineering Simulation (OpenSees 2010) analysis software. Collapse prediction of steel moment frames, which accounts for component deterioration on the basis of the model parameters discussed in this paper, has been validated through comparisons with recent small- and full-scale shaking table collapse tests (Lignos and Krawinkler 2009; Lignos et al. 2011, 2010).

## New Database for Deterioration Modeling of Steel Components

The missing aspect of comprehensive modeling of deterioration characteristics of structural components is the availability of relationships that associate parameters of deterioration models, such as the ones discussed in the previous section, with geometric and material properties and detailing criteria that control deterioration in actual structural elements. To provide information for deterioration model parameters in support of collapse assessment of steel moment-resisting frames, a data collection of component tests is needed in a consistent format that permits validation and calibration of deterioration models. For this purpose, three databases have been developed: (1) wide flange beams, (2) steel tubular sections, and (3) concrete beams. The focus of this paper is in the first database. More information about the other two databases can be found in Lignos and Krawinkler (2009, 2010).

The steel database includes steel W-sections (primarily beams but also a few columns) from Newell and Uang (2006). At this stage of development, the steel W-section database includes more than 300 specimens. The complete set of data together with comprehensive documentation can be downloaded through the Network for Earthquake Engineering Simulation (NEES) central repository (available from https://nees.org/warehouse/project/84).

The database contains data in the following three categories: (1) metadata, which includes (a) distinction based on configuration of beam-to-column subassembly and test setup; (b) connection type, (c) measured material properties of beam and column components, (d) slab details, and (e) report excerpts that contain a qualitative summary for the individual tests; (2) reported results (measurements and observations as reported in test documentation, including digitized hysteretic load-displacement response, moment-rotation response, and panel zone shear-force—distortion

response (if reported); and (3) deduced data (information deduced from metadata and reported data for the purpose of calibration of deterioration models).

The steel W-section database documents experimental data from tests that have been conducted on beam-to-column subassemblies in which inelastic deformations are primarily concentrated in flexural plastic hinge regions of W (or H) sections. The primary deterioration mode of the steel components that develop a plastic hinge is local or lateral torsional buckling. Several cases in which components fail in a brittle mode (e.g., fracture around weldments), and are referred to as nonductile, are included in the database but are not part of any regression analysis discussed subsequently in this paper, since emphasis is on modern connections that are currently used in engineering practice. Various types of beam-to-column connections are employed in the test specimens, with the connection type clearly identified in each entry of the database. About 80 of the specimens have "reduced beam sections" (RBS), in which plastic hinges develop away from the beam-to-column connection.

Cyclic response data of many of the more recent experiments were received from researchers in digitized format. However, more than 40% of the cyclic response data, primarily from older experiments, were received in paper format. Force-deformation responses of these tests had to be manually digitized from research reports. To facilitate this effort, an object-oriented digitization software called Digitizer was developed by Lignos and Krawinkler (2009), which provides all the digital data of interest.

In the evaluation of modeling parameters presented in the subsequent sections, the data of the W-section database are subdivided into RBS data and other-than-RBS data. The latter contained results from tests of various beam-to-column connections in which a plastic hinge in the beam developed at or near the column face, and the pertinent model parameters could be quantified with confidence. Tests in which the connection type clearly affected plastic hinge behavior, such as fracture at beam-to-column weldments or at welded flange plates, were eliminated from consideration. Thus, the other-than-RBS connection types used in the evaluation reflect general plastic hinge behavior in beams and not behavior of individual connection types. For individual connection types, the number of tests is relatively small and the trends are not sufficiently clear to justify parameter quantification on the basis of connection type. For the same reason, only beams without a slab are considered in this evaluation. With these limitations, the focus is on quantification of modeling parameters for moment-rotation relationships with symmetric hysteretic response characteristics. The emphasis in the following discussion is on the deformation parameters  $\theta_p$ ,  $\theta_{pc}$ , and  $\Lambda$ , followed by a brief discussion on the modeling parameters  $M_v$ ,  $M_c/M_v$ ,  $\kappa$ , and  $\theta_u$ .

## **Trends for Deformation Modeling Parameters**

This section illustrates trends that show the dependence of modeling parameters  $(\theta_n, \theta_{nc}, \text{ and } \Lambda)$  on selected geometric properties of steel W sections. Trends are illustrated by plotting data points of a single model parameter against a pertinent geometric parameter. The information presented in the plots (see Figs. 3–6) is obtained from calibrations in which the parameters of the modified IK deterioration model are matched to the experimental momentrotation relationships of the W-sections steel database (e.g., see Fig. 2). A regression line is included in the individual plots to illustrate the overall trends for the modeling parameter, whenever the coefficient of determination,  $R^2$ , is larger than 0.1. The parameter  $R^2$  provides insight into the "goodness" of linear fit assuming that each one of the geometric parameters can be treated as an independent random variable, ignoring the correlation between various geometric parameters. The linear regression lines serve only to illustrate trends; they are not presented for quantitative evaluation of data. The development of multivariate regression equations that account for correlations of geometric and material parameters in the quantification of modeling parameters is discussed subsequently in this paper. Trends for the following four data sets are evaluated:

- 1. Beams with other-than-RBS connections and depth 102 mm (4 in.)  $\leq d \leq 914$  mm (36 in.) (data set 1);
- 2. Beams with RBS connections and depth 457 mm (18 in.)  $\leq d \leq 914$  mm (36 in.) (data set 2);
- 3. Beams with other-than-RBS connections and depth  $d \ge$  533 mm (21 in.) (data set 3); and
- Beams with RBS connections and depth d ≥ 533 mm (21 in.) (data set 4).

Data set 1 contains experiments on small sections, which are useful to observe trends but conceivably deemphasize trends for the sizes of sections used in engineering practice to design a steel moment-resisting frame in a seismic region. This is why data sets 3 and 4 were generated, which are subsets that contain only beams with  $d \ge 533$  mm (21 in.). However, for beams with RBS, there are

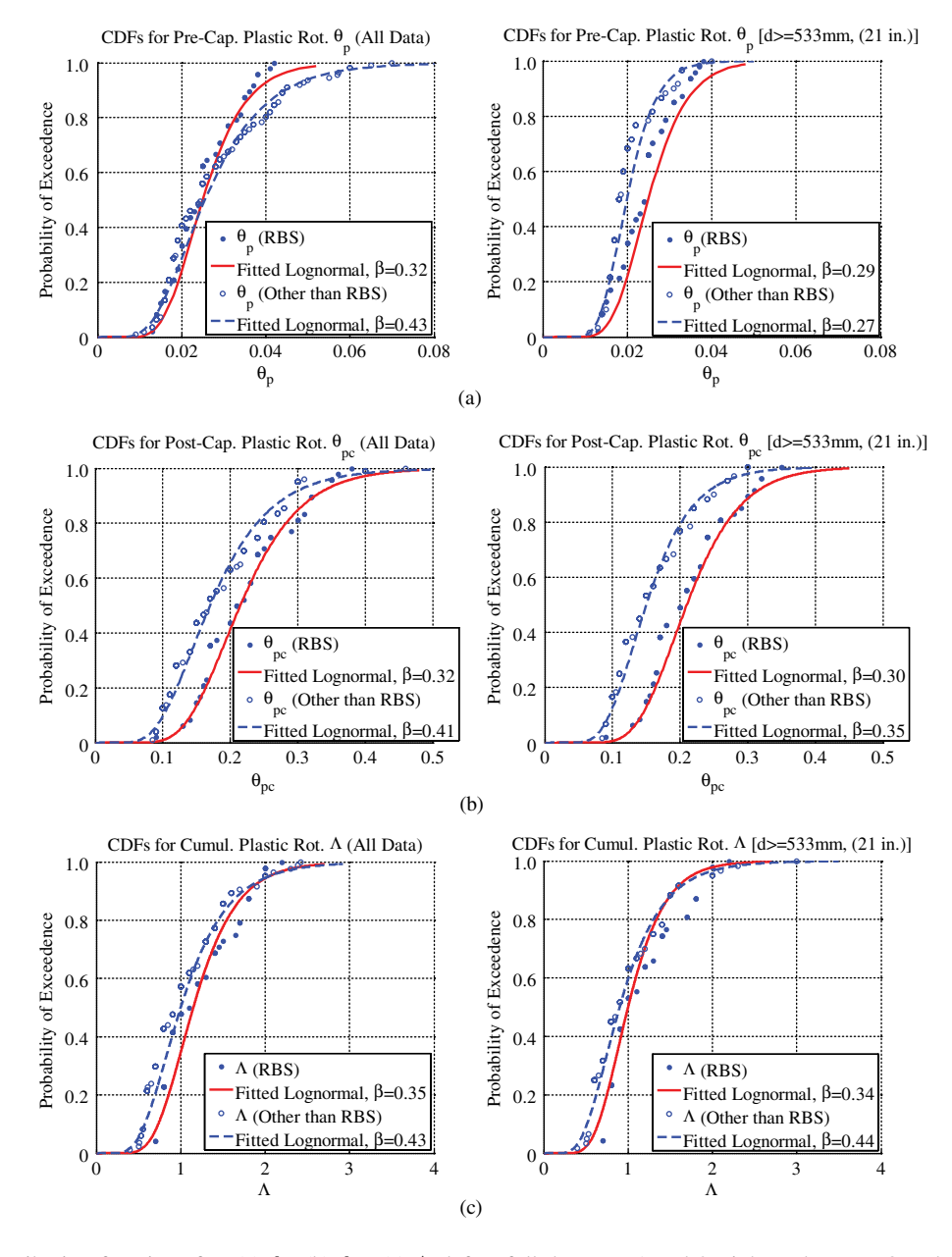
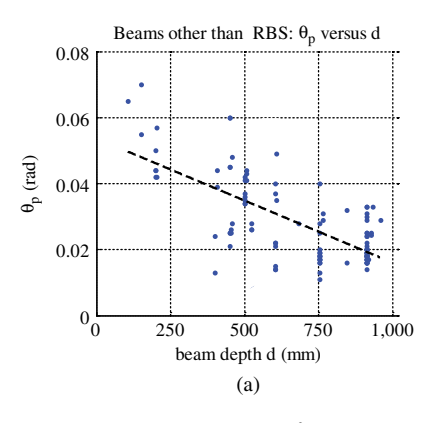
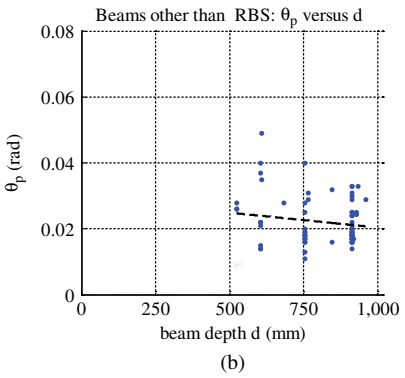
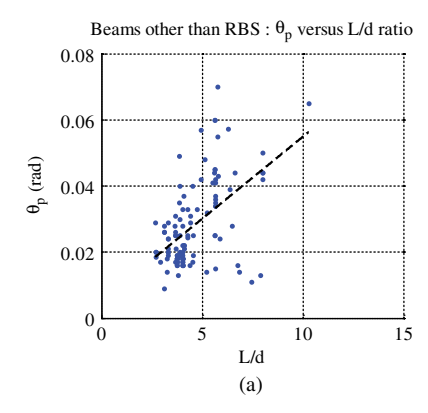


Fig. 3. Cumulative distribution functions for: (a)  $\theta_p$ ; (b)  $\theta_{pc}$ ; (c)  $\Lambda$ ; left = full data sets 1 and 2; right = data sets 3 and 4,  $d \ge 533$  mm (21 in.)





**Fig. 4.** Dependence of plastic rotation  $\theta_p$  on beam depth d for other-than-RBS beams: (a) full data set; (b)  $d \ge 533$  mm (21 in.)



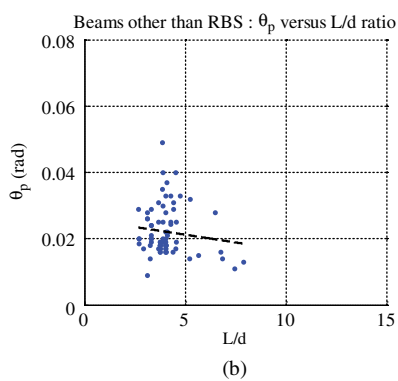


**Fig. 5.** Dependence of plastic rotation  $\theta_p$  on shear span-to-depth ratio L/d for other-than-RBS beams: (a) full data set; (b)  $d \ge 533$  mm (21 in.)

no tests available with  $d \le 457$  mm (18 in.), hence data sets 2 and 4 do not differ by much. Only a few selected plots are presented in this paper. A detailed discussion of trends of component deterioration parameters with respect to geometric and material parameters is presented in Lignos and Krawinkler (2009).

## Statistical Information on Parameters $\theta_p$ , $\theta_{pc}$ , and $\Lambda$

Cumulative distribution functions (CDFs) for  $\theta_p$ ,  $\theta_{pc}$ , and  $\Lambda$  as obtained from the four data sets are shown in Fig. 3. Each plot shows CDFs for other-than-RBS and RBS sections. The CDFs reveal general statistical characteristics but do not display dependencies on individual properties. This information is relevant for detailed studies concerned with quantifying modeling uncertainties and their effect on the collapse capacity of structural systems subjected to earthquake excitations; so far, a systematic collection of experimental data that could be used to document statistical information (median and standard deviation) on deterioration parameters of components was not available. The lognormally distributed CDFs for the four data sets shown in Fig. 3 are comparable, but, in general, the median value of the modeling parameters for beams with other-than-RBS connections is smaller than that for beams with RBS connections. The dispersion is larger for other-than-RBS beams compared with beams with RBS, partially because this set includes experimental data from different connection types.

#### Dependence of Modeling Parameters on Beam Depth d

An increase in beam depth d is associated with a clear decrease in modeling parameters. This is supported by Fig. 4(a), which shows data and a linear regression line for the precapping plastic rotation  $\theta_p$  for data set 1 (full data set for other-than-RBS beams). This data set includes beams with a depth varying from 102 to 914 mm (4 to 36 in.). Others (FEMA 2000a, b) have pointed out the strong dependence of plastic rotation capacity on beam depth. This strong dependence is driven in part by the incorporation of small sections in the database and is not confirmed for the range of primary interest for tall buildings  $[d \ge 533 \text{ mm } (21 \text{ in.})]$  on the basis of Fig. 4(b).

#### Dependence of Modeling Parameters on Shear Span-to-Depth Ratio L/d

On the basis of simple curvature analysis with disregard of local instabilities,  $\theta_p$  of a given beam section is perceived to be linearly proportional to the beam shear span L (distance from plastic hinge location to point of inflection). This perception is supported by the plot in Fig. 5(a), which shows the dependence of  $\theta_p$  on L/d for the full other-than-RBS data set [beams with 102 mm (4 in.)  $\leq d \leq$ 914 mm (36 in.)]. But the strong dependence on L/d is not evident when only beams of depth  $\geq$  533 mm (21 in.) are considered [see Fig. 5(b)]. The reason is that most deep beams are susceptible to a predominance of web buckling and lateral torsional buckling, and both of these susceptibilities increase with a decrease in the moment gradient (more uniform moment, as implied by an increase in the L/d ratio). This phenomenon offsets much of the curvature integration effect for a larger plastic hinge length. On the basis of this information, it is concluded that, for beams with depth  $\geq$ 533 mm (21 in.), a description of beam plastic deformation capacity in terms of a ductility ratio  $\theta_p/\theta_v$  is often misleading because  $\theta_v$ increases linearly with L (for a given beam section) but  $\theta_p$  does not. Assume two cantilever beams made of the same W section. One beam has length L and the other L/2. The yield rotation  $\theta_{v}$  for the first beam with length L will be  $M_v/6EI/L$  and for the second beam with length L/2 will be  $M_{\nu}/(6EI/L/2)$ , i.e.,  $\theta_{\nu}$  linearly increases with length. But the experimental data for set with  $d \ge 533$  mm show that  $\theta_p$  does not depend strongly on L/d

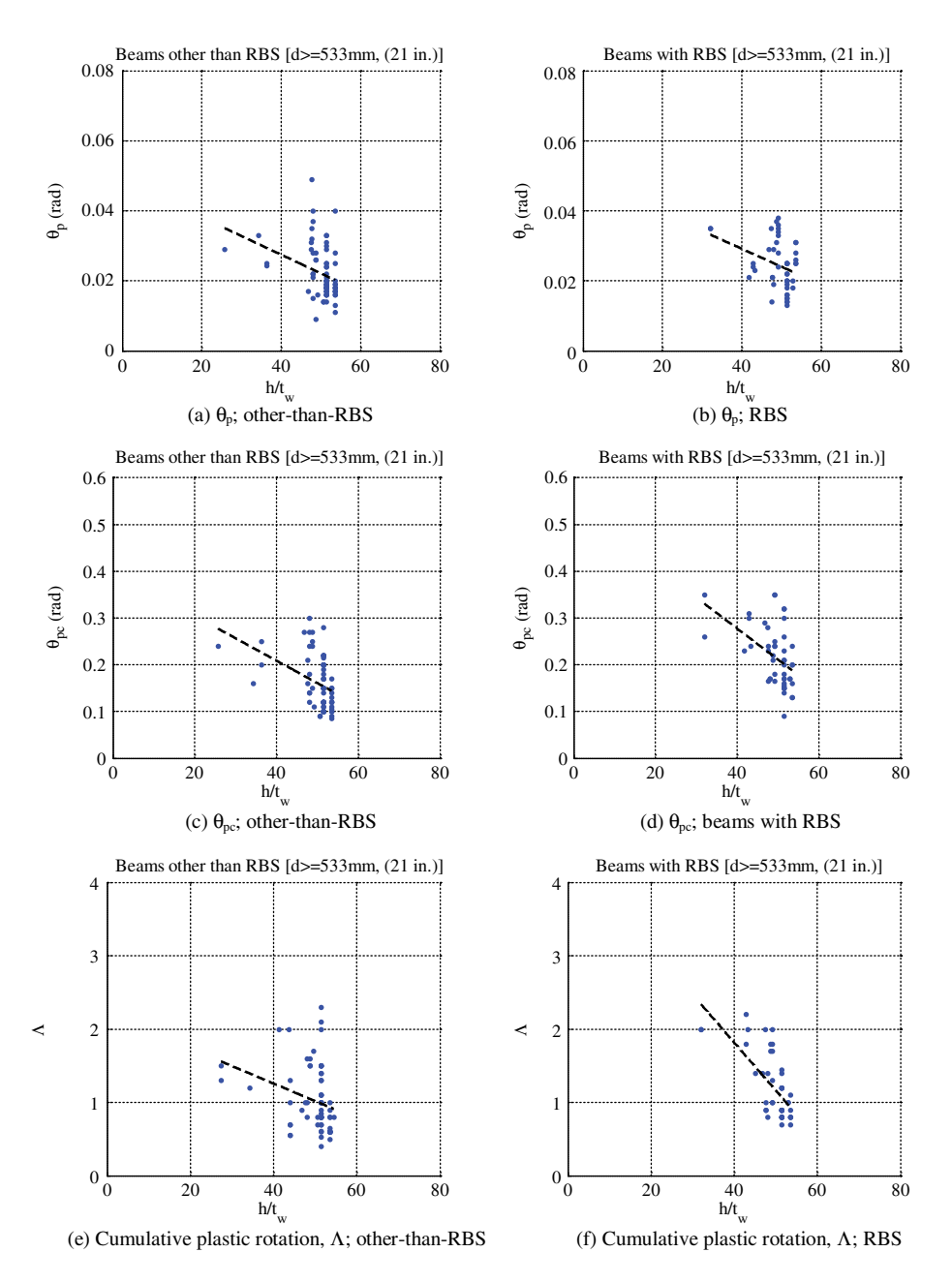


Fig. 6. Dependence of modeling parameters on  $h/t_w$  ratio of beam web,  $d \ge 533\,$  mm (21 in.): (a)  $\theta_p$ , other-than-RBS; (b)  $\theta_p$ , RBS; (c)  $\theta_{pc}$ , other-than-RBS; (d)  $\theta_{pc}$ , beams with RBS; (e) cumulative plastic rotation,  $\Lambda$ , other-than-RBS; (f) cumulative plastic rotation,  $\Lambda$ , RBS

[see Fig. 5(b)]. In other words, the ratio  $\theta_p/\theta_y$  depends strongly on beam span L. Similar observations are made for the parameters  $\theta_{pc}$  and  $\Lambda$ .

#### Dependence of Modeling Parameters on $L_b/r_v$

This ratio is associated with sensitivity to lateral torsional buckling. The parameter  $L_b$  is defined in this case as the distance from the column face to the nearest lateral brace, and  $r_y$  is the radius of gyration about the y-axis of the beam. The American Institute of Steel Construction (2005) requires that this ratio be less than  $2,500/F_y$ . Results from the steel beam database indicate that  $\theta_p$  is somewhat but not greatly affected by  $L_b/r_y$ , provided that the ratio is close to or smaller than the value required by seismic codes. A decrease of  $L_b/r_y$  to 50% of the value required by AISC (2005) increases  $\theta_p$ , on average, by 2.5 and 10% for other-than-RBS beams and beams with RBS, respectively. Providing lateral bracing close

to the RBS portion of a beam decreases the rate of cyclic deterioration, because twisting of the RBS region is delayed. Uang et al. (2000) reached the same conclusion for beams with RBS.

# Dependence of Modeling Parameters on the Width/Thickness Ratio of the Beam Flange $b_{\rm f}/2t_{\rm f}$

When the effect of the  $b_f/2t_f$  ratio on  $\theta_p$  is viewed in isolation, a small  $b_f/2t_f$  ratio has a negligible effect on  $\theta_p$ . For most of the deeper beams in the database, a small  $b_f/2t_f$  implies a narrow wide-flange beam with small radius of gyration  $r_y$  and large fillet-to-fillet web depth over web thickness ratio  $h/t_w$ , both of which have a detrimental effect on  $\theta_p$  because (1) a larger  $h/t_w$  ratio makes a beam more susceptible to web local buckling, and (2) a small  $r_y$  makes a beam more susceptible to lateral torsional buckling. In contrast, the data show a clear benefit of a smaller  $b_f/2t_f$  ratio for the parameters  $\theta_{pc}$  and  $\Lambda$ , since a beam with a smaller

 $b_f/2t_f$  ratio does not develop a large flange local buckle, i.e., postcapping strength deterioration and cyclic deterioration occur at a slower rate.

# Dependence of Modeling Parameters on the Depth-to-Thickness Ratio of the Beam Web $h/t_w$

This geometric parameter is found to be very important for all three modeling parameters (see Fig. 6). The reason is that a beam with a large  $h/t_w$  ratio is more susceptible to web local buckling. This triggers flange local buckling and, at larger inelastic cycles, also triggers lateral torsional buckling (Lay 1965; Lay and Galambos 1966) Fig. 6 indicates also that the trends for all three modeling parameters are similar for RBS and other-than-RBS sections.

# Regression Equations for $\theta_p,\,\theta_{pc},\,$ and $\Lambda,\,$ Accounting for Geometric and Material Properties

In this section, regression equations are proposed to predict deterioration modeling parameters discussed previously. The primary focus is on  $\theta_p$ ,  $\theta_{pc}$ , and  $\Lambda$ . Recommendations for modeling of effective bending strength  $M_y$ , postyield strength ratio  $M_c/M_y$ , residual bending strength  $\kappa$ , and ultimate rotation capacity  $\theta_u$  parameters are also presented.

Lay (1965) and Lay and Galambos (1966) showed that web local buckling is coupled with flange local buckling and lateral torsional buckling. Hence, a nonlinear regression model is used to evaluate the contribution of each important property identified previously to the selected response parameter (RP). The general nonlinear model used is

$$RP = a_1 \cdot (X_1)^{a_2} \cdot (X_2)^{a_3} \dots (X_n)^{a_{n+1}}$$
 (5)

in which  $\alpha_1, \alpha_2, \dots \alpha_{n+1}$  = constants known as regression coefficients; and  $X_1, X_2 \dots X_i$  = predictor variables. On the basis of an evaluation of steel database information and observations on trends discussed partially in the previous section, six parameters are found to primarily affect the deterioration parameters of steel components. Using these six parameters, Eq. (5) becomes

$$RP = a_1 \cdot \left(\frac{h}{t_w}\right)^{a_2} \cdot \left(\frac{b_f}{2 \cdot t_f}\right)^{a_3} \cdot \left(\frac{L_b}{r_y}\right)^{a_4} \cdot \left(\frac{L}{d}\right)^{a_5} \cdot \left(\frac{c_{\text{unit}}^1 \cdot d}{533}\right)^{a_6} \cdot \left(\frac{c_{\text{unit}}^2 \cdot F_y}{355}\right)^{a_7}$$

$$(6)$$

in which  $F_y$  = expected yield strength of the flange of the beam in megapascals, which is normalized by 355 MPa (typical nominal yield strength of European structural steel and equivalent with nominal yield strength of about 50 ksi U.S. steel); and  $c_{\rm unit}^1$  and  $c_{\rm unit}^2$  = coefficients for units conversion. They both are 1.0 if millimeters and megapascals are used, and they are  $c_{\rm unit}^1$  = 25.4 and  $c_{\rm unit}^2$  = 6.895 if d is in inches and  $F_y$  is in ksi, respectively.

Stepwise regression analysis (Chatterjee et al. 2000) is used to develop regression equations for the three model parameters  $\theta_p$ ,  $\theta_{pc}$ , and  $\Lambda$ . Only variables that are statistically significant at the 95% level using a standard t-test and F-test (see Chatterjee et al. 2000) are included in the regression equations presented in the subsequent sections. Variables with insignificant impact are not included in the regression equations. Equations are presented for other-than-RBS beam and beams with RBS. For other-than-RBS beams, two sets of equations are proposed: one for the entire range of data and the other for the data set with  $d \ge 533$  mm (21 in.). For beams with RBS, the regression equations are based on the full set of tests since there are no beams with RBS with d < 457 mm (18 in.) in the W-sections database.

## Precapping Plastic Rotation $\theta_p$

For the full data set for other-than-RBS beams (data set 1), the equation for  $\theta_p$  obtained from multivariate regression analysis using 107 specimens is

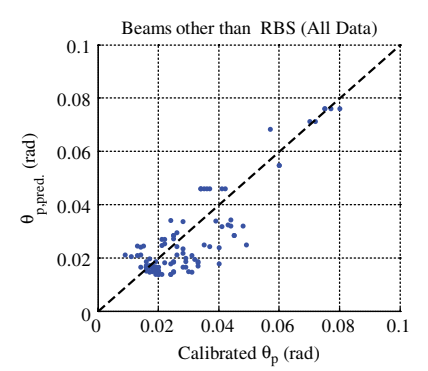
$$\theta_{p} = 0.0865 \cdot \left(\frac{h}{t_{w}}\right)^{-0.365} \cdot \left(\frac{b_{f}}{2 \cdot t_{f}}\right)^{-0.140} \cdot \left(\frac{L}{d}\right)^{0.340} \cdot \left(\frac{c_{\text{unit}}^{1} \cdot d}{533}\right)^{-0.721} \cdot \left(\frac{c_{\text{unit}}^{2} \cdot F_{y}}{355}\right)^{-0.230} R^{2} = 0.505, \qquad \sigma_{\ln} = 0.32$$
(7)

The large values of regression coefficients for web depth over thickness ratio  $h/t_w$ , beam depth d, and span-to-depth ratio L/d confirm trends pointed out previously. Fig. 7(a) shows data points for predictions obtained from Eq. (7) plotted against the data points obtained from experimental results on the basis of the calibration process described previously in this paper.

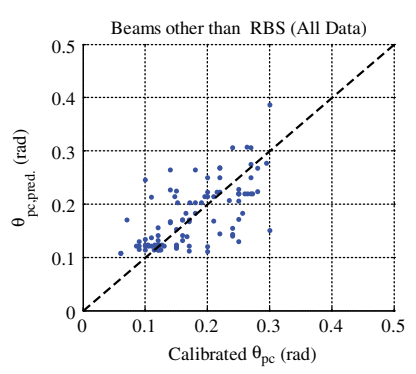
For the data set of beams with  $d \ge 533$  mm (21 in.), the regressed equation for precapping plastic rotation  $\theta_p$ , on the basis of 78 specimens, is given by

$$\begin{split} \theta_p &= 0.318 \cdot \left(\frac{h}{t_w}\right)^{-0.550} \cdot \left(\frac{b_f}{2 \cdot t_f}\right)^{-0.345} \left(\frac{L_b}{r_y}\right)^{-0.0230} \cdot \left(\frac{L}{d}\right)^{0.090} \\ & \cdot \left(\frac{c_{\text{unit}}^1 \cdot d}{533}\right)^{-0.330} \cdot \left(\frac{c_{\text{unit}}^2 \cdot F_y}{355}\right)^{-0.130} \\ R^2 &= 0.457, \qquad \sigma_{\text{ln}} = 0.351 \end{split} \tag{8}$$

In Eq. (8), the effects of d and L/d on  $\theta_p$  are not as significant as in Eq. (7) for the entire range of data, as concluded from the trends plots discussed in the previous section of this paper.



(a) Predicted versus calibrated values of  $\theta_{p}$ 



(b) Predicted versus calibrated values of  $\theta_{pc}$ 

**Fig. 7.** Predicted versus calibrated  $\theta_p$  and  $\theta_{pc}$  parameters for other-than-RBS beams: (a) predicted versus calibrated values of  $\theta_p$ ; (b) predicted versus calibrated values of  $\theta_{pc}$ 

On the basis of 72 test specimens with beams with RBS with  $d \ge 533$  mm (21 in.) the regressed equation for precapping plastic rotation  $\theta_p$  is given by

$$\begin{split} \theta_p &= 0.19 \cdot \left(\frac{h}{t_w}\right)^{-0.314} \cdot \left(\frac{b_f}{2 \cdot t_f}\right)^{-0.100} \cdot \left(\frac{L_b}{r_y}\right)^{-0.185} \cdot \left(\frac{L}{d}\right)^{0.113} \\ &\cdot \left(\frac{c_{\text{unit}}^1 \cdot d}{533}\right)^{-0.760} \cdot \left(\frac{c_{\text{unit}}^2 \cdot F_y}{355}\right)^{-0.0700} \\ R^2 &= 0.56, \qquad \sigma_{\text{ln}} = 0.24 \end{split} \tag{9}$$

Eq. (9) indicates that the effect of  $h/t_w$  and d dominates on plastic rotation capacity  $\theta_p$  of beams with RBS. Uang and Fan (1999) came to similar conclusions regarding the effect of  $h/t_w$  on  $\theta_p$ , on the basis of a data set of 55 RBS specimens and using the difference between the rotations at 80% of the ultimate strength and at yield strength as a definition of plastic rotation capacity.

## Postcapping Plastic Rotation $\theta_{pc}$

For the development of predictive equations for  $\theta_{pc}$ , only specimens with clear indication of postcapping behavior are considered from the W-section database. For other-than-RBS beams, 104 specimens were used. The empirical equation for  $\theta_{pc}$ , obtained from multivariate regression analysis of the full set of other-than-RBS beams, is given by

$$\theta_{pc} = 5.63 \cdot \left(\frac{h}{t_w}\right)^{-0.565} \cdot \left(\frac{b_f}{2 \cdot t_f}\right)^{-0.800} \cdot \left(\frac{c_{\text{unit}}^1 \cdot d}{533}\right)^{-0.280} \cdot \left(\frac{c_{\text{unit}}^2 \cdot F_y}{355}\right)^{-0.430} R^2 = 0.48, \qquad \sigma_{\text{ln}} = 0.25$$
(10)

Predicted versus calibrated  $\theta_{pc}$  values for the total range of data set 1 are presented in Fig. 7(b).

After eliminating specimens with d < 533 mm (21 in.) (data set 3), the proposed empirical equation for  $\theta_{pc}$ , on the basis of 72 specimens, is given by

$$\theta_{pc} = 7.50 \cdot \left(\frac{h}{t_w}\right)^{-0.610} \cdot \left(\frac{b_f}{2 \cdot t_f}\right)^{-0.710} \cdot \left(\frac{L_b}{r_y}\right)^{-0.110} \cdot \left(\frac{c_{\text{unit}}^1 \cdot d}{533}\right)^{-0.161} \cdot \left(\frac{c_{\text{unit}}^2 \cdot F_y}{355}\right)^{-0.320}$$

$$R^2 = 0.49, \qquad \sigma_{\text{ln}} = 0.24 \tag{11}$$

The regression equation for  $\theta_{pc}$  for beams with RBS, on the basis of 61 specimens, is

$$\theta_{pc} = 9.52 \cdot \left(\frac{h}{t_w}\right)^{-0.513} \cdot \left(\frac{b_f}{2 \cdot t_f}\right)^{-0.863} \cdot \left(\frac{L_b}{r_y}\right)^{-0.108} \cdot \left(\frac{c_{\text{unit}}^2 \cdot F_y}{355}\right)^{-0.360} R^2 = 0.48, \quad \sigma_{\text{ln}} = 0.26$$
(12)

Patterns reflected in Eqs. (10)–(12) agree with the ones from previous studies by Axhag (1995) and White and Barth (1998). These researchers proposed empirical equations for predicting the descending slope of the moment-rotation curve of beams and concluded that flange and web local buckling are the primary contributors to the descending slope of the beams.

#### Reference Cumulative Plastic Rotation $\Lambda$

As discussed previously, the reference cumulative plastic rotation  $\Lambda$  is a parameter that defines the rate of cyclic deterioration. The specimens considered for the development of predictive equations for  $\Lambda$  are the ones that fail in a ductile manner and for which cyclic deterioration is clearly observed. All modes of cyclic deterioration are assumed to be defined by the same  $\Lambda$ . The exponent c of Eq. (3) is kept equal to 1.0 for the sake of simplicity.

Eq. (13) is the best-fit multivariate regression equation for predicting the cumulative rotation capacity  $\Lambda$  for the full set of other-than-RBS beams on the basis of 85 specimens with clear indication of cyclic deterioration:

$$\Lambda = \frac{E_t}{M_y} = 495 \cdot \left(\frac{h}{t_w}\right)^{-1.34} \cdot \left(\frac{b_f}{2 \cdot t_f}\right)^{-0.595} \cdot \left(\frac{c_{\text{unit}}^2 \cdot F_y}{355}\right)^{-0.360}$$

$$R^2 = 0.484, \qquad \sigma_{\text{ln}} = 0.35 \tag{13}$$

Eq. (13) indicates that the geometric parameter d, L/d, and  $L_b/r_y$  become statistically insignificant. The reason why the  $L_b/r_y$  ratio has a small effect on  $\Lambda$  is that all the specimens included in the multivariate regression analysis satisfy the AISC (2005) lateral bracing requirements. The small effect of  $L_b/r_y$  was also pointed out by Roeder (2002).

For the data set of beams with nominal depth larger than 533 mm (21 in.) the following equation is derived to predict  $\Lambda$  (66 specimens showed clear indication of cyclic deterioration):

$$\Lambda = \frac{E_t}{M_y} = 536 \cdot \left(\frac{h}{t_w}\right)^{-1.26} \cdot \left(\frac{b_f}{2 \cdot t_f}\right)^{-0.525} \cdot \left(\frac{L_b}{r_y}\right)^{-0.130} \cdot \left(\frac{c_{\text{unit}}^2 \cdot F_y}{355}\right)^{-0.291} R^2 = 0.496, \qquad \sigma_{\text{ln}} = 0.34$$
(14)

The proposed equation for predicting the cumulative rotation capacity  $\Lambda$  for beams with RBS, on the basis of 55 specimens, is

$$\Lambda = \frac{E_t}{M_y} = 585 \cdot \left(\frac{h}{t_w}\right)^{-1.14} \cdot \left(\frac{b_f}{2 \cdot t_f}\right)^{-0.632} \cdot \left(\frac{L_b}{r_y}\right)^{-0.205} \cdot \left(\frac{c_{\text{unit}}^2 \cdot F_y}{355}\right)^{-0.391}$$

$$R^2 = 0.486, \qquad \sigma_{\text{ln}} = 0.35$$
(15)

Uang et al. (2000) have shown that beams with RBS are susceptible to twisting at the RBS region because of the reduced flanges, and additional lateral bracing reduces the rate of strength deterioration at large deformation levels because it reduces the lateral buckling amplitude near the RBS location. Roeder (2002) came to the same conclusion. This is reflected in the exponent of the  $L_b/r_v$  term in Eq. (15).

Experimental data with the following range of parameters are used in deriving Eqs. (7)–(15):

- $20 \le h/t_w \le 55$  for other-than-RBS;  $21 \le h/t_w \le 55$  for RBS;
- $20 \le L_b/r_v \le 80$  for other-than-RBS;  $20 \le L_b/r_v \le 65$  for RBS;
- $4 \le b_f/2t_f \le 8$  for other-than-RBS;  $4.5 \le b_f/2t_f \le 7.5$  for RBS;
- $2.5 \le L/d \le 7$  for other-than-RBS;  $2.3 \le L/d \le 6.3$  for RBS;
- 102 mm (4 in.)  $\leq d \leq 914$  mm (36 in.) for other-than-RBS; 533 mm (21 in.)  $\leq d \leq 914$  mm (36 in.) for RBS; and
- 240 MPa (35 ksi)  $\leq F_y \leq$  450 MPa (65 ksi) for other-than-RBS; 262 MPa (38 ksi)  $\leq F_y \leq$  435 MPa (63 ksi) for RBS.

The specimens included in the steel database were fabricated from three main types of steel material: A36, A572, Grade 50, and A992, Grade 50. The yield strength values reported in this

paper are the ones obtained from actual coupon tests conducted by the experimentalists.

The range of validity of the regression equations is only as good as the experimental data allows it to be. The data do not include heavy W14 sections (heavier than W14  $\times$  370) and heavy (heavier than W36  $\times$  150) and deep (e.g., deeper than W36) beam sections. The predictions from the regression equations have been compared with data from the only series of experiments found in the literature on heavy W14 sections (Newell and Uang 2006) and have been found to provide reasonably close values of experimentally obtained modeling parameters. Until more tests on columns become available, the preceding equations provide the best estimates that can be offered for columns.

Tables 1 and 2 summarize the variation of deterioration parameters for other-than RBS beams and beams with RBS, respectively, for a range of sections (W21 to W36) that satisfy seismic compactness criteria. The range of deterioration parameter values is also reflected in the cumulative distribution functions of these parameters presented in Fig. 3. Sections whose geometric or material properties are slightly outside the range of properties, on which the predictive equations are based, are noted.

#### Effective Yield Strength M<sub>v</sub>

As noted previously, the modified IK deterioration model does not account for cyclic hardening, but the effect of isotropic hardening is incorporated approximately by increasing the yield moment (bending strength) to an effective value  $M_y$  that accounts for isotropic hardening on average. The effective yield strength typically is larger by a small amount than the predicted bending strength  $M_{y,p}$ , which is defined as the plastic section modulus Z times the measured material yield strength obtained from coupon tests. Table 3 summarizes the mean and standard deviation of  $M_y/M_{y,p}$  ratios for other-than-RBS beams and beams with RBS. For the latter,  $M_{y,p}$  is defined on the basis of the reduced section properties.

Options exist for more refined modeling that account explicitly for combined isotropic and kinematic hardening (e.g., Sivaselvan and Reinhorn 2000; Jin and El-Tawil 2003). Such options were not incorporated to keep the model relatively simple for engineering implementation.

#### Postyield Strength Ratio M<sub>c</sub>/M<sub>v</sub>

Postyield hardening, and subsequently  $M_c$ , is described by the ratio of the maximum moment on the backbone curve shown in Fig. 1(a) over the effective yield bending strength,  $M_y$ , discussed previously. The  $M_c/M_y$  and  $\theta_c/\theta_y$  ratios define the strain hardening stiffness of the backbone curve shown in Fig. 1(a). This stiffness is important because of its effect on the  $P-\Delta$  stability of a structural system (Medina and Krawinkler 2003). Table 3 summarizes statistics (mean and standard deviation) of  $M_c/M_y$  for RBS and

Table 1. Modeling Parameters for Various Beam Sizes (Other-than-RBS) Based on Regression Equations

Section size	$\theta_p$ (rad)	$\theta_{pc}$ (rad)	Λ	$h/t_w$	$b_f/2t_f$	$L_b/r_y$	L/d	d (mm)
W21 × 62	0.031	0.14	0.90	46.90	6.70	50.00	7.14	533
$W21 \times 147$	0.038	0.22	2.23	26.10	5.43	50.00	6.79	561
$W24 \times 84$	0.028	0.15	1.00	45.90	5.86	50.00	6.22	612
$W24 \times 207$	0.034	0.28	2.81	24.80	4.14	50.00	5.84	653
$W27 \times 94$	0.024	0.13	0.83	49.50	6.70	50.00	5.58	683
$W27 \times 217$	0.029	0.22	2.14	28.70	4.70	50.00	5.28	721
$W30 \times 108$	0.021	0.12	0.82	49.60	6.91	50.00	5.03	757
$W30 \times 235$	0.024	0.19	1.76	32.20	5.03	50.00	4.79	795
$W33 \times 130$	0.019	0.11	0.79	51.70	6.73	50.00	4.53	841
$W33 \times 241$	0.021	0.16	1.42	35.90	5.68	50.00	4.39	869
$W36 \times 150$	0.017	0.12	0.81	51.90	6.38	50.00	4.18	912
$W36 \times 210$	0.020	0.18	1.45	39.10	4.49	50.00	4.09	932

Note: Assumed beam shear span L = 3,810 mm (150 in.);  $L_b/r_v = 50$ ; and expected yield strength  $F_v = 379$  MPa (55 ksi).

Table 2. Modeling Parameters for Various Beam Sizes (Beams with RBS) Based on Regression Equations

Section size	$\theta_p$ (rad)	$\theta_{pc}$ (rad)	Λ	$h/t_w$	$\frac{\mathcal{E}}{b_f/2t_f}$	$L_b/r_y$	L/d	d (mm)
W21 × 62	0.028	0.16	0.97	46.90	6.70	50.00	7.14	533
$W21 \times 147$	0.033	0.27	2.15	26.10	5.43	50.00	6.79	561
$W24 \times 84$	0.026	0.19	1.08	45.90	5.86	50.00	6.22	612
$W24 \times 207$	$0.030^{a}$	$0.34^{a}$	2.71 <sup>a</sup>	24.80	4.14	50.00	5.84	653
$W27 \times 94$	0.022	0.16	0.91	49.50	6.70	50.00	5.58	683
$W27 \times 217$	$0.026^{a}$	$0.29^{a}$	2.12 <sup>a</sup>	28.70	4.70	50.00	5.28	721
$W30 \times 108$	0.020	0.16	0.89	49.60	6.91	50.00	5.03	757
$W30 \times 235$	0.023	0.25	1.78	32.20	5.03	50.00	4.79	795
$W33 \times 130$	0.018	0.16	0.86	51.70	6.73	50.00	4.53	841
$W33 \times 241$	0.020	0.22	1.46	35.90	5.68	50.00	4.39	869
$W36 \times 150$	0.017	0.16	0.89	51.90	6.38	50.00	4.18	912
$W36 \times 210$	$0.019^{a}$	$0.25^{a}$	1.53 <sup>a</sup>	39.10	4.49	50.00	4.09	932

Note: Assumed beam shear span L = 3,810 mm (150 in.);  $L_b/r_v = 50$ ; and expected yield strength  $F_v = 379$  MPa (55 ksi).

<sup>a</sup>Values slightly outside the range of experimental data.

**Table 3.** Statistics of Ratios of Effective-to-Predicted Component Yield Strength and Capping Strength-to-Effective Yield Strength

Connection type	Mean $M_y/M_{y,p}$	$\sigma_{My/My,p}$	Mean $M_c/M_y$	$\sigma_{Mc/My}$
RBS	1.06	0.12	1.09	0.03
Other-than-RBS	1.17	0.21	1.11	0.05

other-than-RBS connections on the basis of information extracted from the database of steel components. In general,  $M_c/M_y$  is a more stable parameter to describe postyield strength increase than the traditional strain hardening ratio because the latter depends strongly on yield rotation, which, in turn, depends strongly on the beam span selected in the experiment, i.e., on the moment gradient. Experimental data used in this study have shown that the strength increase beyond yielding is much less sensitive to the moment gradient than the yield rotation, which is linearly proportional to the beam span.

## Residual Strength Ratio κ

Low-cycle fatigue experimental studies (Krawinkler et al. 1983; Ricles et al. 2004) indicate four ranges of cyclic deterioration. The first range has negligible deterioration in which local instabilities have not yet occurred or are insignificant. The second range involves an almost constant rate of cyclic deterioration attributable to continuous growth of local buckles. In the third range, deterioration proceeds at a very slow rate because of the stabilization in buckle size; this range is associated with the residual strength of a steel component. These three ranges are followed by a range of very rapid deterioration, which is caused by crack propagation at local buckles (ductile tearing). From the data sets for W-sections, a residual strength ratio  $\kappa = M_r/M_v$  of approximately 0.4 is suggested for sets 3 and 4. This value is based on a relatively small set of data points from which an estimate of  $\kappa$  could be made with confidence. To assess residual strength more reliably, more experiments with very large deformation cycles need to be conducted.

#### Ultimate Rotation Capacity $\theta_u$

At very large inelastic rotations, cracks may develop in the steel base material close to the apex of the most severe local buckle, and rapid crack propagation will then occur, followed by ductile tearing and essentially complete loss of strength [see Ricles et al. (2004) for illustrations and end of last loading cycle of the experimental data shown in Fig. 2(b)]. The modified IK deterioration model captures this failure mode with the ultimate rotation capacity  $\theta_{\mu}$ . This rotation depends on the loading history and may be very large for cases in which only a few very large cycles are executed (e.g., near-fault loading history or ratcheting type of global behavior) as discussed in Uang et al. (2000) and Lignos and Krawinkler (2009). Estimates of  $\theta_u$  are made in this paper only for experiments with stepwise increasing cycles of the type required in the AISC (2005) seismic specifications. For other-than-RBS beams, an estimate of  $\theta_u$  is 0.05 to 0.06 rad on the basis of available data from various researchers (Allen et al. 1996; Ricles et al. 2000). For beams with RBS, an estimate of  $\theta_u$  is 0.06 to 0.07 rad (Engelhardt et al. 2000; Ricles et al. 2004). For monotonic type of loading  $\theta_u$ is on the order of three times as large as the  $\theta_u$  values reported in the preceding sections for symmetric cyclic loading protocols. Ductile tearing is not found to be critical in analytical studies in which the collapse capacity of a steel moment-resisting frame has been evaluated, because steel frame structures usually approach their collapse capacity before ductile tearing occurs (Ibarra and Krawinkler 2005; Lignos and Krawinkler 2009; NIST 2010; Lignos et al. 2010, 2011).

#### **Conclusions**

This paper is concerned with deterioration modeling of steel components from a recently developed database on experimental studies of wide flange beams. The database of more than 300 specimens contains, in consistent format, extensive information of worldwide experimental data on components that have been subjected to monotonic and cyclic loading. The steel database can serve for validation and improvement of deterioration models used for collapse assessment of steel moment-resisting frames. On the basis of statistical evaluation of calibrated moment-rotation diagrams obtained from tests included in this database and with the use of multivariate regression analysis, empirical equations are proposed that predict the deterioration modeling parameters  $\theta_p$ ,  $\theta_{pc}$ , and  $\Lambda$  of beams with reduced beam sections and other-than-RBS beams. Quantitative information for modeling of effective yield moment  $M_{\nu}$ , postyield strength ratio  $M_c/M_v$ , residual strength ratio  $\kappa$ , and ultimate rotation capacity  $\theta_u$  is also provided. From available trend plots, cumulative distribution functions on deterioration parameters, and predictive equations, the main conclusions are the following:

- The median value of the precapping plastic rotation  $\theta_p$  is on the order of 0.02 rad, the median of postcapping rotation capacity  $\theta_{pc}$  is on the order of 0.20 rad, and the median of the reference cumulative rotation capacity  $\Lambda$  is on the order of 1.0 rad.
- For all the connection types evaluated, the primary contributor
  to the deterioration parameters θ<sub>p</sub>, θ<sub>pc</sub>, and Λ is the beam web
  depth h over thickness ratio h/t<sub>w</sub>. Of some importance is the
  effect of flange width to thickness ratio b<sub>f</sub>/2t<sub>f</sub>, beam depth
  d, and shear span over beam depth ratio L/d.
- For sections used commonly in modern steel moment-resisting frames  $[d \geq 533 \text{ mm } (21 \text{ in.})]$ , a description of beam deformation capacity in terms of a ductility capacity ratio  $\theta_p/\theta_y$  is misleading because  $\theta_y$  increases linearly with L (for a given beam section) but  $\theta_p$  does not.
- Experimental data indicate that deterioration modeling parameters are not very sensitive to the beam span (i.e., the length of the plastic hinge regions.
- Closely spaced lateral bracing (small  $L_b/r_y$  ratio) increases  $\theta_p$ ,  $\theta_{pc}$ , and  $\Lambda$ , but not by a large amount (provided that the  $L_b/r_y$  ratio does not exceed an upper limit on the order of 70). The effect of  $L_b/r_y$  on  $\Lambda$  of beams with RBS is somewhat more important compared to other-than-RBS beams, particularly when additional bracing is installed near the RBS location.
- The effective yield strength  $M_y$  used in the modified Ibarra-Krawinkler model, which accounts for cyclic hardening, is about 1.10 times the plastic moment  $M_{y,p}$  obtained from plastic section modulus times actual material yield strength for both other-than-RBS beams and beams with RBS.
- The postyield strength ratio  $M_c/M_y$  is, on average, 1.10 for both other-than-RBS beams and beams with RBS. It is found that the ratio  $M_c/M_y$  together with the ratio  $\theta_p/\theta_y$  provide a much better definition of the postyield stiffness than the traditional strain hardening ratio.
- A reasonable estimate of residual strength is 0.4 times the
  effective yield strength M<sub>y</sub>. More experiments with very large
  deformation cycles are needed to assess residual strength with
  high confidence.
- Ultimate rotation capacity θ<sub>u</sub> of steel components that fail in a
  ductile manner is strongly dependent on loading history. For
  components subjected to symmetric cyclic loading histories,
  θ<sub>u</sub> is on the order of 0.06 rad, but it is about three times as large
  when the component is subjected to a near-fault loading protocol or to monotonic loading.

The conclusions in this paper are drawn on the basis of interpretation of experimental data. Detailed analytical validation studies have not been performed. The data are available for such studies at https://nees.org/warehouse/project/84.

#### Acknowledgments

This study is based on work supported by the U.S. National Science Foundation (NSF) under Grant No. CMS-0421551 within the George E. Brown, Jr. Network for Earthquake Engineering Simulation (NEES) Consortium, and by a grant from the CUREE-Kajima Phase VI joint research program. This financial support is gratefully acknowledged. The authors would like to thank graduate students Yash Ahuja, Guillermo Soriano, Richard Weiner, and Yavor Yotov for their invaluable assistance in the steel database development. Any opinions, findings, and conclusions or recommendations expressed in this paper are those of the authors and do not necessarily reflect the views of sponsors.

#### References

- American Institute of Steel Construction (AISC). (2005). Seismic provisions for structural steel buildings, including supplement No. 1, Chicago.
- Allen, J., Partridge, J. E., and Richard, R. M. (1996). "Stress distribution in welded/bolted beam to column moment connections." *Internal Rep.*, Seismic Structural Design Association, Inc., Los Angeles
- Axhag, F. (1995). "Plastic design of composite bridges allowing for local buckling." *Rep. 95-09T*, Lulea Univ. of Technology, Lulea, Sweeden.
- Baber, T., and Noori, M. N. (1985). "Random vibration of degrading, pinching systems." *J. Eng. Mech.*, 111(8), 1010–1026.
- Berry, M., Parrish, M., and Eberhard, M. (2004). *PEER structural performance database user's manual*, Pacific Engineering Research Center, Univ. of California, Berkeley, CA, 38.
- Bouc, R. (1967). "Forced vibration of mechanical systems with hysteresis." Abstract Proc., 4th Conference on Nonlinear Oscillations, Academia, Prague, Czechoslovakia.
- Casciati, F. (1989). "Stochastic dynamics of hysteretic media." Struct. Saf., 6, 259–269.
- Chatterjee, S., Hadi, A. S., and Price, B. (2000). Regression analysis by example, 3rd Ed., Wiley, New York.
- Dennis, J. E. Jr. (1977). *Nonlinear least-squares, state of the art in numerical analysis*, D. Jacobs, ed., Academic Press, 269–312.
- Engelhardt, M. D., Fry, D. T., and Venti, M. J. (2000). "Behavior and design of radius cut reduced beam section connections." *Rep. No.* SAC/BD-00/17, SAC Joint Venture, Sacramento, CA.
- Federal Emergency Management Agency (FEMA). (2000a). "Recommended seismic design criteria for new steel moment frame buildings." *Rep. FEMA 350*, Washington, DC.
- Federal Emergency Management Agency (FEMA). (2000b). "Prestandard and commentary for the seismic rehabilitation of buildings." *Rep. FEMA 356*, Washington, DC.
- Federal Emergency Management Agency (FEMA). (2009). "Quantification of building seismic performance factors." *Rep. FEMA P695*, Washington, DC.
- Haselton, C. B., and Deierlein, G. G. (2007). "Assessing seismic collapse safety of modern reinforced concrete moment frames." Rep. No. TB 157, John A. Blume Earthquake Engineering Center, Stanford Univ., Stanford, CA.
- Ibarra, L. F., and Krawinkler, H. (2005). "Global collapse of frame structures under seismic excitations." Rep. No. TB 152, The John A. Blume Earthquake Engineering Center, Stanford Univ., Stanford, CA.
- Ibarra, L. F., Medina, R., and Krawinkler, H. (2002). "Collapse assessment of deteriorating SDOF systems." Proc. 12th European Conf. on Earthquake Engineering, Paper 665, Elsevier Science, London.
- Ibarra, L. F., Medina, R. A., and Krawinkler, H. (2005). "Hysteretic models that incorporate strength and stiffness deterioration." *Earthquake Eng. Struct. Dyn.*, 34(12), 1489–1511.

- Iwan, W. D. (1966). "A distributed-element model for hysteresis and its steady-state dynamic response." J. Appl. Mech., 33(4), 893–900.
- Jin, J., and El-Tawil, S. (2003). "Inelastic cyclic model for steel braces." J. Eng. Mech., 129(5), 548–557.
- Krawinkler, H., Zohrei, M., Irvani, B. L., Cofie, N., and Tamjed, H. H. (1983). "Recommendations for experimental studies on the seismic behavior of steel components and materials." *Rep. No. TB 61*, The John A. Blume Earthquake Engineering Center, Stanford Univ., Stanford, CA
- Lay, M. G. (1965). "Flange local buckling in wide-flange shapes." J. Struct. Div., 91(ST6), 95–116.
- Lay, M. G., and Galambos, T. V. (1966). "Bracing requirements for inelastic steel beams." J. Struct. Div., 92(ST2), 207–228.
- Lignos, D. G., Hikino, T., Matsuoka, Y., and Nakashima, M. (2010). "Collapse assessment of steel moment frames based on E-defense full scale shake table collapse tests." Proc., 13th Japan Earthquake Engineering Symp., Japanese Association for Earthquake Engineering, Tokyo.
- Lignos, D. G., and Krawinkler, H. (2007). "A database in support of modeling of component deterioration for collapse prediction of steel frame structures." Proc. ASCE Structures Congress, SEI institute, Long Beach, CA.
- Lignos, D. G., and Krawinkler, H. (2009). "Sidesway collapse of deteriorating structural systems under seismic excitations." *Rep. No. TB 172*, The John A. Blume Earthquake Engineering Center, Stanford Univ., Stanford, CA.
- Lignos, D. G., and Krawinkler, H. (2010). "A steel database for component deterioration of tubular hollow square steel columns under varying axial load for collapse assessment of steel structures under earthquakes." Proc. 7th Int. Conf. on Urban Earthquake Engineering (7CUEE), Center for Urban Earthquake Engineering, Tokyo Institute of Technology, Tokyo.
- Lignos, D. G., Krawinkler, H., and Whittaker, A. S. (2011). "Prediction and validation of sidesway collapse of two scale models of a 4-story steel moment frame." *Earthquake Eng. Struct. Dyn.*, 40(7), 807–825.
- Ma, F., Ng, C. H., and Ajavakom, N. (2006). "On system identification and response prediction of degrading structures." *Struct. Contr. Health Monit.*, 13(1), 347–364.
- Medina, R., and Krawinkler, H. (2003). "Seismic demands for nondeteriorating frame structures and their dependence on ground motions." Rep. No. TB 144, The John A. Blume Earthquake Engineering Center, Stanford Univ., Stanford, CA.
- Medsker, L. R., and Jain, L. C. (2000). Recurrent neural networks: Design and applications, CRC Press, Boca Raton, FL.
- Mostaghel, N. (1999). "Analytical description of pinching, degrading hysteretic systems." *J. Eng. Mech.*, 125(2), 216–224.
- National Institute of Standards and Technology (NIST). (2010). Evaluation of the FEMA P695 methodology for quantification of building seismic performance factors, Gaithersburg, MD.
- Newell, J., and Uang, C. M. (2006). "Cyclic behavior of steel columns with combined high axial load and drift demand." Rep. No. SSRP-06/22, American Institute of Steel Construction, Inc, Dept. of Structural Engineering, Univ. of California, San Diego.
- OpenSees. (2010). "Open system for earthquake engineering simulation." Pacific Earthquake Engineering Research Center (PEER), (http://opensees.berkeley.edu) (Dec. 15, 2010).
- Otani, S. (1981). "Hysteresis models of reinforced concrete for earthquake response analysis." J. Faculty of Engineering, Univ. of Tokyo, Series A, XXXVI(2), 407–441.
- Prakash, V., Powell, G. H., and Campbell, S. (1993). "DRAIN-2DX: Basic program description and user guide." *Rep. No. UCB/SEMM-1993/17*, University of California, Berkeley, CA, 97.
- Rahnama, M., and Krawinkler, H. (1993). "Effect of soft soils and hysteresis models on seismic design spectra." Rep. No. TB 108, The John A. Blume Earthquake Engineering Center, Stanford Univ., Stanford, CA.
- Reinhorn, A. M., Madan, A., Valles, R. E., Reichmann, Y., and Mander, J. B. (1995). "Modeling of masonry infill panels for structural analysis." *Rep. NCEER-95-0018*, State Univ. of New York at Buffalo, Buffalo, NY.

- Ricles, J. M., Mao, C., Lu, L. W., and Fisher, J. W. (2000). "Development and evaluation of improved ductile welded unreinforced flange connections." *Rep. No. SAC/BD-00/24.*, SAC Joint Venture, Sacramento, CA.
- Ricles, J. M., Zhang, X., Lu, L. W., and Fisher, J. (2004). "Development of seismic guidelines for deep-column steel moment connections." *Rep. No. 04-13*, Advanced Technology for Large Structural Systems, Lehigh Univ., Bethlehem, PA.
- Roeder, C. W. (2002). "General issues influencing connection performance." J. Struct. Eng., 128(4), 420–428.
- Sivaselvan, M., and Reinhorn, A. M. (2000). "Hysteretic models for deteriorating inelastic structures." J. Eng. Mech. Div., 126(6), 633–640.
- Sivaselvan, M., and Reinhorn, A. M. (2006). "Lagrangian approach to structural collapse simulation." *J. Eng. Mech.*, 132(8), 795–805.
- Song, J., and Pincheira, J. (2000). "Spectral displacement demands of stiffness and strength degrading systems." *Earthquake Spectra*, 16(4), 817–851.
- Uang, C. M., and Fan, C. C. (1999). "Cyclic instability of steel moment connections with reduced beam sections." Rep. No. SSRP-99/21, Dept. of Structural Engineering. Univ. of California, San Diego.
- Uang, C. M., Kent-Yu, K., and Gilton, C. (2000). "Cyclic response of RBS moment connections: Loading sequence and lateral bracing effects."

- Rep. No. SSRP-99/13, Univ. of California at San Diego, La Jolla, CA. Vamvatsikos, D., and Cornell, C. A. (2002). "Incremental dynamic analysis." Earthquake Eng. Struct. Dyn., 31(3), 491–514.
- Wen, Y.-K. (1980). "Equivalent linearization for hysteretic systems under random excitation." J. Appl. Mech., 47(1), 150–154.
- White, D. W., and Barth, K. E. (1998). "Strength and ductility of compact flange *I*-girders in negative bending." *J. Constr. Steel Res.*, 45(3), 241–280.
- Yun, G. Y., Ghaboussi, J., and Elnashai, A. S. (2007). "Modeling of hysteretic behavior of beam-column connections based on selflearning simulation." *Rep. Mid-America Earthquake Center*, Dept. of Civil and Environmental Engineering, Univ. of Illinois at Urbana-Champaign, Urbana, IL.
- Zareian, F., and Krawinkler, H. (2009). "Simplified performance based earthquake engineering." *Rep. No. TB 169*, The John A. Blume Earthquake Engineering Research Center, Stanford Univ., Stanford, CA.
- Zareian, F., Lignos, D. G., and Krawinkler, H. (2010). "Evaluation of seismic collapse performance of steel special moment resisting frames using ATC-63 methodology." *Proc. Structures Congress*, ASCE, New York.